

# ネットワークパス上の複数区間の利用可能帯域計測手法

鯉谷 和正<sup>†</sup> 長谷川 剛<sup>††</sup> 村田 正幸<sup>†</sup>

<sup>†</sup> 大阪大学 大学院情報科学研究科 〒565-0871 大阪府吹田市山田丘 1-5

<sup>††</sup> 大阪大学 サイバーメディアセンター 〒560-0043 大阪府豊中市待兼山町 1-32

E-mail: <sup>†</sup>{k-koitani,murata}@ist.osaka-u.ac.jp, <sup>††</sup>hasegawa@cmc.osaka-u.ac.jp

**あらまし** エンド端末間のネットワークパスの利用可能帯域計測に関する既存研究は、ボトルネック区間の利用可能帯域の値を推定することができるが、ボトルネック箇所の特定制や、ネットワークパス上の複数区間の利用可能帯域を個別に計測することはできない。本稿では、エンド端末間のパス上における複数区間における利用可能帯域を同時に計測する手法を提案する。提案手法は、経路上のルータにおいてパケットの到着時間が記録できることを前提とし、各ネットワーク区間におけるパケット到着間隔の変化を利用し、利用可能帯域を推定する。性能評価の結果、送信端末に近いネットワーク区間より、受信端末に近いネットワーク区間の利用可能帯域が大きい場合においても、それぞれの区間の利用可能帯域を高い精度で計測することが可能であることを示す。

**キーワード** 利用可能帯域、能動的計測、エンド間パス計測、ルータ、タイムスタンプ

## An Available Bandwidth Measurement Method for Arbitrary Parts of End-to-End Path

Kazumasa KOITANI<sup>†</sup>, Go HASEGAWA<sup>††</sup>, and Masayuki MURATA<sup>†</sup>

<sup>†</sup> Graduate School of Information Science and Technology, Osaka University  
Yamadaoka 1-5, Suita, Osaka, 565-0871 Japan

<sup>††</sup> Cybermedia Center, Osaka University  
Machikaneyama-cho 1-32, Toyonaka, Osaka, 560-0043 Japan

E-mail: <sup>†</sup>{k-koitani,murata}@ist.osaka-u.ac.jp, <sup>††</sup>hasegawa@cmc.osaka-u.ac.jp

**Abstract** Existing techniques for measuring available bandwidth measure the available bandwidth at bottlenecks along the path, and most of them do not specify the bottleneck location. In this report, we propose an end-to-end measurement method for the hop-by-hop available bandwidth along a network path. Such a technique can facilitate advanced traffic control, especially in heterogeneous network environments. The proposed method assumes a situation where intermediate routers can record the arrival and departure times of incoming packets as timestamps in the packets themselves. The endhost sends probe packets at various rates and estimates the available bandwidth at each network section using the incoming and outgoing rates of packets calculated from intermediate timestamps, based on statistical processing under a fluid traffic model. We present extensive simulation results for the proposed method and confirm that it can accurately measure the available bandwidth of each section along the network path even when the available bandwidth of the sender-side network is smaller than that of the receiver-side network.

**Key words** Available bandwidth, active probing, end-to-end measurement, router, timestamp

## 1. Introduction

The available bandwidth of an end-to-end network path is determined by bottlenecks, which are the section with the smallest available bandwidth along the path. Many tools for measuring the available bandwidth of an end-to-end network path are proposed [1–8] and evaluated [9–11]. These bandwidth measurement tools can determine the available bandwidth at bottlenecks, but with the exception of *pathneck* [12], none of them can determine the location of the bottlenecks along the path. However, knowing the locations of bottlenecks may enhance the quality of network applications. For example, in overlay networks for video and voice conferencing, when an endhost determines the location of a bottleneck link, the endhost can enhance the application quality by adding or deleting overlay nodes to the overlay network to change the route between endhosts. Another example is network control in wired-cum-wireless network environments, where a wireless client terminal can control the data transmission rate of the wireless network according to the measured bandwidth of the wired part. However, to our knowledge, there has been no previous research on such end-to-end measurement of the available bandwidth of multiple sections of the network path.

In this paper, we propose an end-to-end measurement method for the hop-by-hop available bandwidth of a network path. The proposed method estimates the available bandwidth based on the assumption that some intermediate routers along the path can record the arrival and departure times of traversing packets as timestamps in the packets themselves. We divide the end-to-end path into multiple sections at such intermediate routers and estimate the available bandwidth of each section simultaneously by observing the intervals of incoming and outgoing packets in each section. Considering the effect of cross traffic, the endhost sends probe packets at various rates and estimates the available bandwidth based on their incoming and outgoing packet rates at each section. To estimate the available bandwidth, we construct a simple mathematical model of the relationships between incoming and outgoing packet rates.

To evaluate the performance of the proposed method, we conduct simulation experiments using ns-2 [13]. We evaluate the measurement accuracy of the proposed method under various bandwidth settings including situations where the available bandwidth of the sender-side network is smaller than that of the receiver-side network. We also evaluate the performance of the proposed method in several scenarios constructed by varying the settings of physical and available bandwidth and the hop count of the path, and verify the robustness of the proposed method.

The rest of this paper is organized as follows. Section 2. explains the principle of hop-by-hop bandwidth measurement and verifies its feasibility. Subsequently, we propose a multi-section measurement of the available bandwidth. Section 3. evaluates the measurement accuracy of the proposed method in various situations. In Section 4., we conclude this paper and outline the direction of future work.

## 2. Hop-by-hop bandwidth measurement principle and proposed method

We assume that the network path between a sender and a receiver is divided into multiple sections at intermediate routers, as illustrated in Figure 1. Sections of the path from the sender are referred as the 1st, 2nd, ..., Nth network section. The physical bandwidth of the  $j$ th network section is denoted as  $C(j)$ , and the available bandwidth is denoted as  $A(j)$ , assuming that the physical and available bandwidths of each network section remain unchanged during the measurement task. We focus on measuring the available bandwidth for all network sections by using probe packets sent from the sender to the receiver.

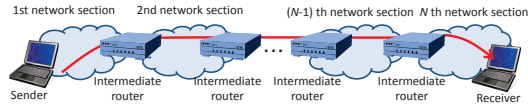


Fig 1: Network model for multi-section bandwidth measurement of the network path

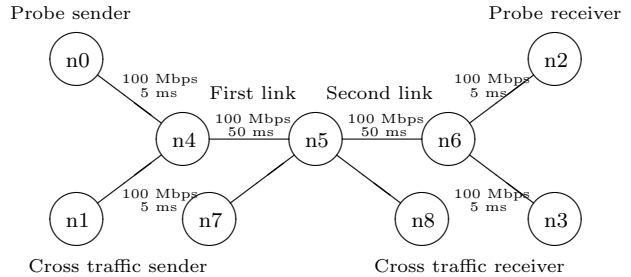


Fig 2: Network topology used in the simulation experiments in Subsection 2.1

### 2.1 Feasibility of multi-section measurement

The available bandwidth of a single network section can be measured by injecting probe packets into the network section at various rates, both higher and lower than the actual available bandwidth of that network section. When all of the injection rates of probe packets are lower than the actual available bandwidth, we cannot measure the available bandwidth accurately. Therefore, to measure the available bandwidth of all network sections along the path, we consider the following condition must be satisfied.

$$\min_{1 \leq k < j} A(k) > A(j) \quad (1 \leq j \leq N) \quad (1)$$

Conversely, measuring the available bandwidth is impossible when the available bandwidth of the  $j$ th network section is smaller than that of the  $(j + 1)$ th network section because the rate at which probing packets leaves a certain network section is expected to be equal to or lower than the available bandwidth of that section. However, when probing packets are injected at a sufficiently high rate, the outgoing rate would become higher than the actual available bandwidth of that network section [14]. This means that it is feasible to measure the available bandwidth of individual network sections even when Equation (1) is not satisfied. In the following subsection, we validate the feasibility of the proposed method by simulation experiments using ns-2.

Figure 2 shows the network topology used in the simulation experiments. The propagation delay of the link between  $n4$  and  $n5$  (First link) and that between  $n5$  and  $n6$  (Second link) is 50 ms, and that between all other links is 5 ms. The physical bandwidth of all links in the network is set to 100 Mbps. Cross traffic is sent from node  $n1$  to node  $n8$  via nodes  $n4$  and  $n5$  at a rate of  $X_1$  Mbps, as well as from node  $n7$  to node  $n3$  via nodes  $n5$  and  $n6$  at a rate of  $X_2$  Mbps. Therefore, the available bandwidth of the first link is  $(100 - X_1)$  Mbps and that of the second link is  $(100 - X_2)$  Mbps. The cross traffic consists of UDP packets whose departure intervals follows an exponential distribution with a given mean value. Probe packets are sent from node  $n0$  to node  $n2$  via nodes  $n4$ ,  $n5$ , and  $n6$ , traversing the first and second links. The probe packets are sent from node  $n0$  at intervals from  $1.0 \times 10^{-4}$  to  $2.0 \times 10^{-3}$  s in units of  $1.0 \times 10^{-5}$  s, which corresponds to a rate from 6 Mbps to 120 Mbps. The number of probe packets sent at a time is  $K$ . The probe packet size is set to 1,500 Bytes and the packet size of cross traffic is set to 1,000 Bytes. With these settings, we observe the incoming and

outgoing rates of probe packets at the second link, which are taken as the averaged values over  $K_0$  probe packets.

Figure 3 shows the simulation results for the relationship between incoming and outgoing rates of probe packets at the second link when  $K_0 = 2, 6,$  and  $10$ . This graph shows the case where  $X_1 = 50$  and  $X_2 = 30$ . Since the actual available bandwidth of the first and second links is 50 and 70 Mbps, respectively, Equation (1) is not satisfied. However, we can see from this figure that a non-negligible portion of probe packets are injected into the second link at a rate higher than 50 Mbps, regardless of the value of  $K_0$ . Also, when the incoming rate is high, the outgoing rate of probe packets tends to be lower than the incoming rate, especially if  $K_0$  is large. This means that we can measure the available bandwidth of the second link, even though Equation (1) is not satisfied.

Next, we focus on the effect of  $K_0$ . In the case of small  $K_0$  (Figure 3(a)), there is no stable relationship between incoming and outgoing rates of probe packets. In contrast, too large a value of  $K_0$  would result in smooth incoming and outgoing rates, which would obscure the difference between the two, as can be seen by comparing Figures 3(b) and 3(c). This may affect the measurement accuracy, which is confirmed in Section 3.. Furthermore, a larger value of  $K_0$  requires a larger number of probe packets in order to obtain a sufficient number of probing samples. Thus, when setting the value of  $K_0$ , we must consider the measurement accuracy and the number of probe samples necessary in order to obtain meaningful measurement results.

## 2.2 Proposed method

We propose a method for measuring available bandwidth of multiple sections of an end-to-end network path based on the observations in Subsection 2.1. We first show the principle of the proposed method considering a difference between the measurement of the available bandwidth at the bottleneck and the multi-section measurement. Next, we describe the process of measuring the available bandwidth of arbitrary sections of a network path. Finally, we present the steps in the measurement process in detail.

### 2.2.1 Overview

To measure the available bandwidth of arbitrary sections of a network path, the probe packets have to arrive at each network section at a designated rate. However, this is difficult to achieve in practice for an arbitrary network section because the packet arrival intervals vary due to fluctuation in the amount of cross traffic. For this reason, the sender sends probe packets at various rates to the receiver and estimates the available bandwidth of arbitrary sections of the network path based on statistical analysis. The measurement process is as follows.

- (1) The sender sends probe packets to the receiver at various rates, and intermediate routers along the path record the arrival time of each probe packet as a timestamp into the packet itself.
- (2) When a probe packet arrives at the receiver, the receiver estimates the available bandwidth of each network section based on the arrival and departure times of the probe packet for the corresponding section.
- (3) When the available bandwidth estimation for the entire network is complete or measurement with high accuracy seems to be impossible, the measurement procedure is terminated. Otherwise, we return to step 1.

In the following subsections, we explain steps 1 and 2 in detail.

### 2.2.2 Hop-by-Hop timestamps of probe packets

The bandwidth measurement method presented in this paper is based on the observation of a single pair of incoming and outgoing rates of probe packets in the network. Existing measurement methods can obtain only the available

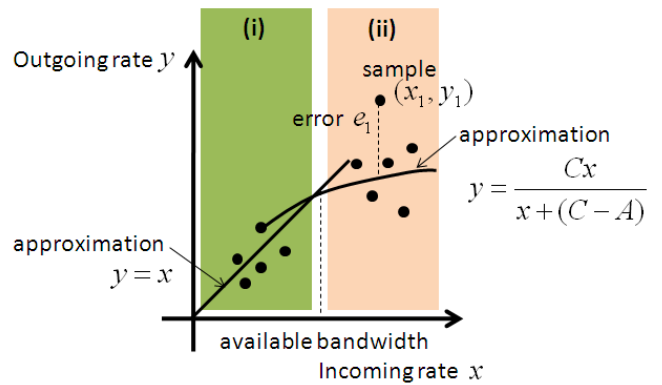


Fig 4: Computation of available bandwidth in the proposed method

bandwidth at bottlenecks in the network. To measure the available bandwidth of multiple network sections, we assume that intermediate routers (Figure 1) can record the times at which probe packets pass through the router into the packets themselves. The proposed method utilizes those timestamps to estimate the available bandwidth of each network section. To our knowledge, routers currently deployed in real-world networks are not capable of recording timestamps into packets, but such routers are being developed [15, 16] for various end-to-end measurement purposes.

### 2.2.3 Calculation of available bandwidth based on statistical analysis

We propose a method for calculating the available bandwidth based on probing results as shown in Figure 3. The simulation results in Figure 3 can be abstracted into a simple mathematical model illustrated in Figure 4. The probing results can be divided into two regions (denoted as (i) and (ii)). In region (i), the departure rate of probe packets is lower than the actual available bandwidth. Therefore, the incoming and outgoing rates become almost equal in that region. In contrast, in region (ii), the probing packets are injected at a higher rate than the actual available bandwidth. In this case, the outgoing rate would be lower than the incoming rate. We utilize a fluid model [10] to determine the outgoing rate of probe packets from the incoming rates and the actual available bandwidth. We denote the incoming rate of probe packets as  $x$  bps and the outgoing rate for that incoming rate as  $y(x)$  bps. The physical available bandwidths are denoted as  $C$  [bps] and  $A$  [bps], respectively. Then, the model in Figure 4 can be represented as follows.

$$y(x) = \begin{cases} x & x \leq A \\ \frac{Cx}{x+(C-A)} & x > A \end{cases} \quad (2)$$

The proposed method first gathers probing samples as shown in Figure 3 and determines the available bandwidth (which corresponds to  $A$  in Equation (2)), by simple regression of the equation to obtain a fit for all probing samples. This regression is the point where the proposed method differs from the train of packet pairs method [17]. We explain the proposed method in detail below.

The sender sends  $K$  probe packets, denoted as  $P_1, P_2, \dots, P_K$ , at a certain rate. We focus on  $K_0$  successive packets beginning with the  $i$ th packet, which corresponds to the sequence  $P_i, P_{i+1}, \dots, P_{i+K_0-1}$  ( $1 \leq i \leq K - K_0 + 1$ ). We calculate the incoming and outgoing rates from timestamps recorded at intermediate routers, which are denoted as  $x_i$  bps and  $y_i$  bps, respectively. We define  $(x_i, y_i)$  as the  $i$ th probing sample. Note that we can obtain  $(K - K_0 + 1)$  samples from  $K$  packets. We assume that the sender sends probing packets repeatedly and obtains  $N_{all}$  samples. Next, we divide these samples based on their incoming rates to obtain the average

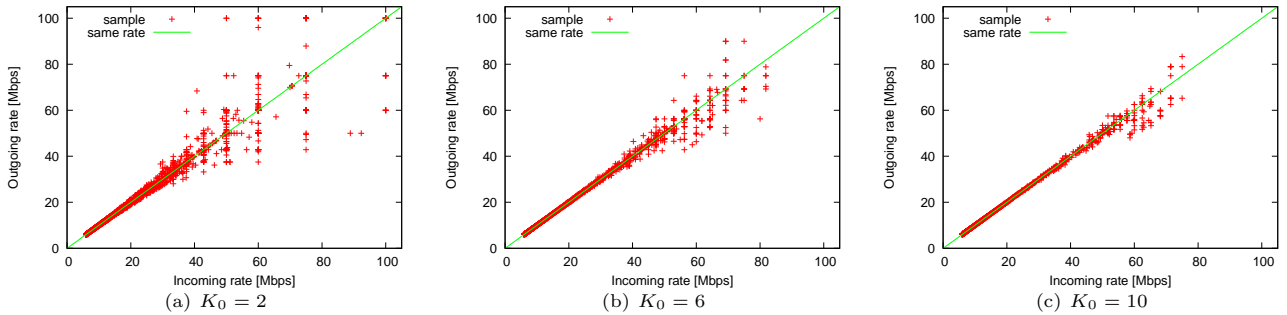


Fig 3: Relationship between incoming and outgoing rates with  $X_1 = 50$  and  $X_2 = 30$

values. We set the rate resolution to  $R_0$  bps. Then, we calculate the average incoming and outgoing rates of samples for each incoming rate. We denote the averaged samples as  $(\hat{x}_k, \hat{y}_k)$  ( $1 \leq k \leq \lceil C(j)/R_0 \rceil$ ), assuming that  $C(j)$  is known in advance, and estimate the available bandwidth of the  $j$  th network section (denoted by  $\bar{A}(j)$ ) by the equation below.

$$\bar{A}(j) = \underset{A(j)}{\operatorname{argmin}} e(A(j)) \quad (3)$$

where  $e(A(j))$  is calculated as follows.

$$e(A(j)) = \sum_{\hat{x}_i \leq A(j)} (\hat{y}_i - \hat{x}_i)^2 + \sum_{\hat{x}_i > A(j)} \left( \hat{y}_i - \frac{C(j) \cdot \hat{x}_i}{\hat{x}_i + (C(j) - A(j))} \right)^2 \quad (4)$$

### 3. Performance evaluation

We evaluate the performance of the proposed method by conducting simulation experiments using ns-2. First, we evaluate the fundamental performance using a 2-hop network topology considering the situation where the available bandwidth of the receiver-side network is higher than that of the sender-side network. Next, we evaluate the influence of various conditions to assess the robustness of the proposed method.

#### 3.1 Fundamental evaluation of the proposed method

First, we examine the basic behavior of the proposed method with a simple network topology. The network topology (illustrated in Figure 2) is the same as in Subsection 2.1. In this topology, the path between the endhosts consists of segments that are not measured (links directly connected to the endhosts) and segments that are measured (all other links). The physical bandwidth of all links is set to 100 Mbps. The available bandwidth of the first link, which is located between nodes n4 and n5, is denoted as  $A(1)$ , and the available bandwidth of the second link, which is located between nodes n5 and n6, is denoted as  $A(2)$ . We vary  $A(1)$  and  $A(2)$  from 10 Mbps to 90 Mbps by changing the rate of cross traffic. The timer granularity of the intermediate router is set to  $1.0 \times 10^{-6}$  s. In this environment, we measure the available bandwidth of the second link by the proposed method.

Figure 5 presents the simulation results for the measurement accuracy of the available bandwidth of the second link. Each graph in Figure 5 corresponds to a different value of the actual available bandwidth of the first link ( $A(1)$ ). The graphs present the relation between actual and estimated values of the available bandwidth of the second link for  $K_0 = 2, 4, 8, 16, 32$  and  $47$ . The values of parameters  $K$  and  $R_0$  of the proposed method are set to 50 and 1 Mbps, respectively. The center of each error bar in the graph indicates the average of the corresponding estimation result, and the width of

each bar indicates 95% confidence interval.

These figures indicate that the available bandwidth of the second link is measured accurately regardless of the actual available bandwidth of the two links ( $A(1)$  and  $A(2)$ ). Especially when  $A(2) < A(1)$ , in which case Equation (1) is satisfied, the available bandwidth can be measured with high accuracy. When  $A(2) > A(1)$ , in which case Equation (1) is not satisfied, the measurement accuracy is lower but remains reasonable. However, when  $A(2)$  is close to 100 Mbps, the measurement accuracy degrades, especially when  $A(1)$  is small. This is due to the decrease in the number of probing samples whose incoming rate is higher than  $A(2)$ . Also, to obtain accurate measurement results, we should avoid setting  $K_0 = 2$  since in that case the measurement results fluctuate considerably (Figure 5). This is because the relation between incoming and outgoing rates becomes unstable (Figure 3(a)).

#### 3.2 Influence of physical bandwidth

We evaluate the influence of physical bandwidth on the measurement accuracy by using the same network topology as in the previous simulation experiments. The difference from the previous experimental setup is the values of the physical and available bandwidths of all links in the network. The physical bandwidth is set to 10 Mbps or 1 Gbps, and the cross traffic rates and available bandwidths are configured proportionally to the physical bandwidth.

Figure 6 presents the simulation results for the available bandwidth of the second link where the physical bandwidth is set to 10 Mbps. We focus on the measurement results for the same bandwidth utilization of the first and second links in Figures 5, and 6. Note that the results for 1 Gbps of physical bandwidth has similar tendency in terms of the measurement accuracy. This figure indicates that the available bandwidth can be measured accurately regardless of the physical bandwidth. In general, when the physical bandwidth is large, the measurement accuracy is low because of the timer granularity of the intermediate router. However, in the proposed method, the statistical processing can compensate for the low measurement accuracy.

#### 3.3 Influence of hop count along path

Next, we evaluate the influence of the hop count along a path on the measurement accuracy. The model for 5-hop network is shown in Figure 7. 3-hop and 9-hop networks have similar topologies except that the number of hops between nodes connecting source and destination hosts is set to three, and nine, respectively. The remaining settings are the same as in the two-hop model.

The above results indicate that the measurement accuracy depends mainly on whether Equation (1) is satisfied. For this reason, we examine the following two cross traffic scenarios.

- Scenario 1: The available bandwidth decreases gradually in equal steps from the sender host to the receiver host.
  - Scenario 2: The available bandwidth increases gradually in equal steps from the sender host to the receiver host.
- The detailed settings for the available bandwidth are summarized in Table 1. The estimation results are shown in



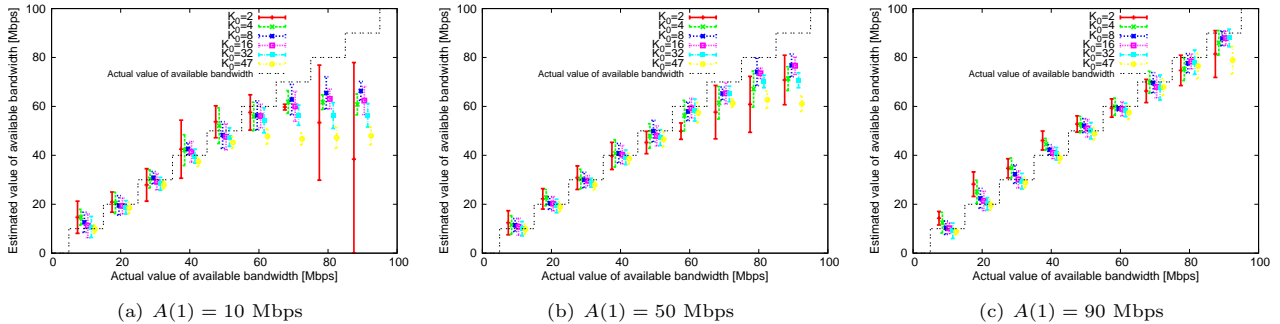


图 5: Estimation results with 100 Mbps of physical bandwidth

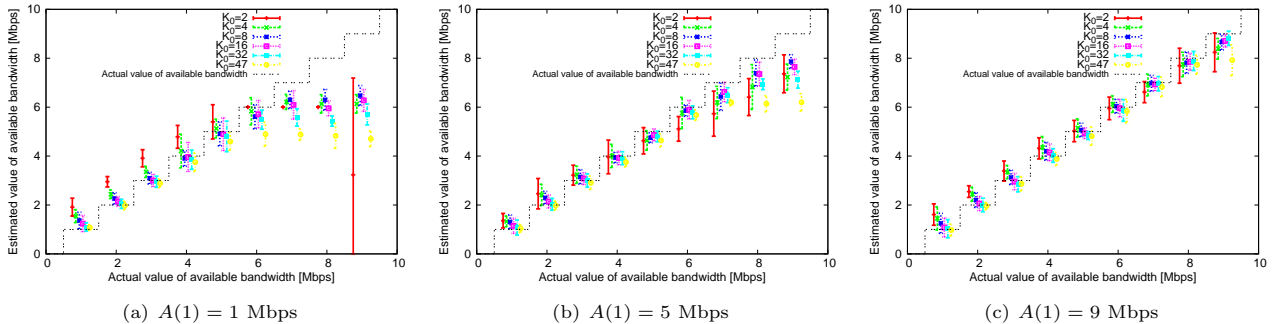


图 6: Estimation results with 10 Mbps of physical bandwidth

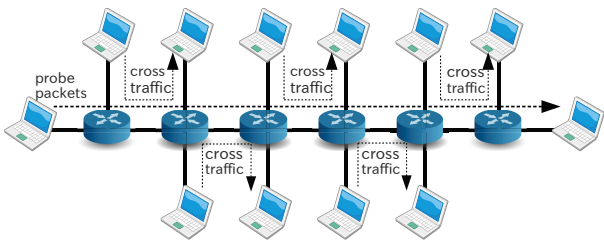


图 7: 5-hop network topology

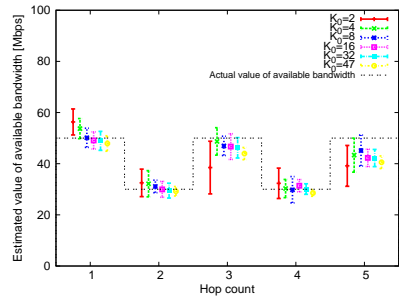


图 10: Estimation results in a case of multiple bottlenecks

表 1: Settings for the available bandwidth in 3-, 5-, and 9-hop topologies

|                | Scenario 1             | Scenario 2             |
|----------------|------------------------|------------------------|
| 3-hop topology | (90, 50, 10) Mbps      | (10, 50, 90) Mbps      |
| 5-hop topology | (90, 70, ..., 10) Mbps | (10, 30, ..., 90) Mbps |
| 9-hop topology | (90, 80, ..., 10) Mbps | (10, 20, ..., 90) Mbps |

Figures 8 and 9 for Scenarios 1 and 2, respectively. Each graph in the figures corresponds to a different hop count of the path. Figure 8 indicates that when the available bandwidth increases together with the hop count from the sender (in which case Equation (1) is satisfied), the available bandwidth can be measured accurately regardless of the total number of hop counts between the sender and the receiver. However, Figure 9 indicates that in case Equation (1) is not satisfied, the estimation accuracy degrades as the hop count from the sender increases. This occurs because when probe packets traverse multiple links with ever smaller available bandwidth, their incoming rates in the subsequent network sections decreases with higher probability.

### 3.4 Performance in case of multiple bottlenecks

Finally, we verify the performance of the proposed method in case of multiple bottleneck locations along the path. We utilize the 5-hop network topology shown in Figure 7. The

physical bandwidth of the links is set to 100 Mbps and the available bandwidth of each link from the sender is 50, 30, 50, 30, and 50 Mbps in this order. The estimation results (Figure 10) indicate that the available bandwidth of all links along the path is measured accurately and the bottleneck locations are identified correctly, suggesting that the proposed method can be applied with equal success in cases of a single or multiple bottleneck locations.

## 4. Conclusion and future work

In this paper, we proposed a method for simultaneous measurement of the available bandwidth at multiple locations along an end-to-end network path. We extended the measurement principle utilized in existing measurement tools by adding a timestamp function to intermediate routers along the path, whereby the arrival and departure times of each packet are recorded in the packet itself. We validated the performance of the proposed method by simulation experiments and found that the available bandwidth at multiple locations along the path can be measured with reasonable accuracy, even when the available bandwidth of the receiver-side network is higher than that of the sender-side network. We also validated the robustness of the proposed method for various situations.

In future work, we plan to introduce an algorithm allow-

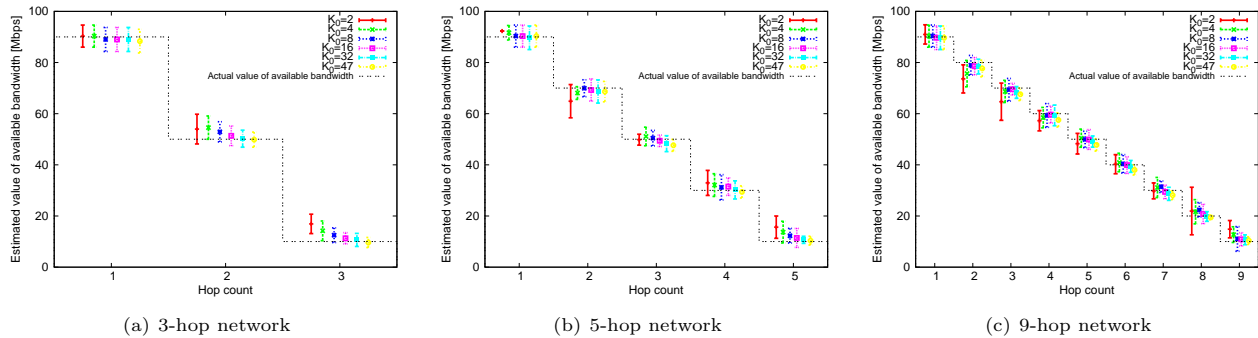


Fig. 8: Effect of hop count in Scenario 1

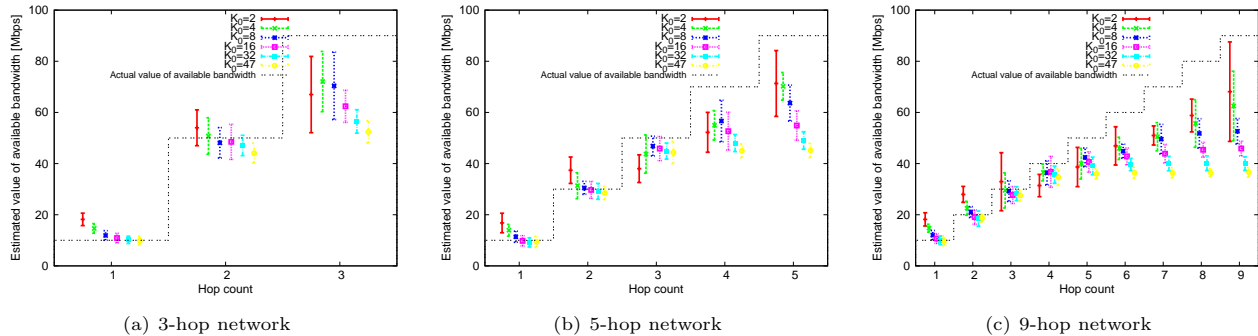


Fig. 9: Effect of hop count in Scenario 2

ing the number of probe packets to be configured in order to decrease the measurement load on the network while maintaining the measurement accuracy. Furthermore, we plan to implement the proposed method and to verify its effectiveness in actual network environments.

#### 文献

- [1] C. Robert L and M. E. Crovella, "Dynamic Server Selection using Bandwidth Probing in Wide-Area Networks," tech. rep., Boston University, 1996.
- [2] M. Jain and C. Dovrolis, "End-to-End Available Bandwidth: Measurement Methodology, Dynamics, and Relation with TCP Throughput," in *Proceedings of ACM SIGCOMM 2002*, pp. 295–308, August 2002.
- [3] V. J. Ribeiro, R. H. Riedi, R. G. Baraniuk, J. Navratil, and L. Cottrell, "pathChirp: Efficient Available Bandwidth Estimation for Network Paths," in *Proceedings of PAM 2003*, pp. 1–11, April 2003.
- [4] A. B. Downey, "Using Pathchar to Estimate Internet Link Characteristics," in *Proceedings of ACM SIGCOMM 1999*, pp. 241–250, October 1999.
- [5] E. Bergfeldt, S. Ekelin, and J. M. Karlsson, "Real-time Available-Bandwidth Estimation using Filtering and Change Detection," *Computer Networks*, vol. 53, no. 15, pp. 2617–2645, October 2009.
- [6] L. Lao, C. Dovrolis, and M. Y. Sanadidi, "The Probe Gap Model can Underestimate the Available Bandwidth of Multihop Paths," *ACM SIGCOMM Computer Communication Review*, vol. 36, no. 5, pp. 29–34, October 2006.
- [7] X. Hei, B. Bensaou, and D. H. K. Tsang, "Model-based End-to-End Available Bandwidth Interference using Queuing Analysis," *Computer Networks*, vol. 50, no. 12, pp. 1916–1937, August 2006.
- [8] T. G. Sultanov and A. M. Sukhov, "Simulation Technique for Available Bandwidth Estimation," in *Proceedings of EMS 2010*, pp. 490–495, November 2010.
- [9] N. Hu and P. Steenkiste, "Evaluation and Characterization of Available Bandwidth Probing Techniques," *IEEE Journal on Selected Areas in Communications*, vol. 21, no. 6, pp. 879–894, August 2003.
- [10] J. Strauss, D. Katabi, and F. Kaashoek, "A Measurement Study of Available Bandwidth Estimation Tools," in *Proceedings of IMC 2003*, pp. 39–44, October 2003.
- [11] A. Shriram, M. Murray, Y. Hyun, N. Brownlee, A. Broido, M. Fomenkov, and K. Claffy, "Comparison of Public End-to-End Bandwidth Estimation Tools on High-Speed Links," in *Proceedings of PAM 2005*, pp. 306–320, March 2005.
- [12] N. Hu, L. E. Li, Z. M. Mao, P. Steenkiste, and J. Wang, "Locating Internet Bottlenecks: Algorithms, Measurements, and Implications," in *Proceedings of ACM SIGCOMM 2004*, pp. 41–54, September 2004.
- [13] "ns-2 web page." available at <http://isi.edu/nsnam/ns/>.
- [14] C. Dovrolis, P. Ramanathan, and D. Moore, "What do Packet Dispersion Techniques Measure?," in *Proceedings of INFOCOM 2001*, vol. 2, pp. 905–914, April 2001.
- [15] A. Machizawa, H. Toriyama, T. Iwama, and A. Kaneko, "Development of a Cascadable Passing Through Precision UDP Time-Stamping Device," *IEICE Transactions on Communications*, vol. J88-B, no. 10, pp. 2002–2011, October 2005. (in Japanese).
- [16] A. Machizawa and Y. Kitaguchi, "Improvement of Software Timestamp Accuracy with Interrupt Handler and High Precision PC," *IEICE Transactions on Communications*, vol. J87-B, no. 10, pp. 1678–1685, October 2004. (in Japanese).
- [17] B. Melander, M. Bjorkman, and P. Gunningberg, "A New End-to-End Probing and Analysis Method for Estimating Bandwidth Bottlenecks," in *Proceedings of GLOBECOM 2000*, vol. 1, pp. 415–421, November 2000.